

Testing AdS/CFT with flavours on a computer

Veselin Filev

work with D. O'Connor

Dublin Institute for Advanced Studies

eNLarge Horizons

1 AdS/CFT correspondence

- Original form
- Adding flavours
- Computer simulations of holographic gauge theories

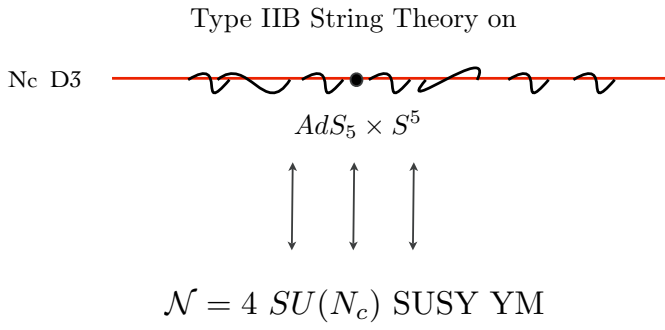
2 BFSS matrix model

- Properties
- Simulation
- Sign Problem

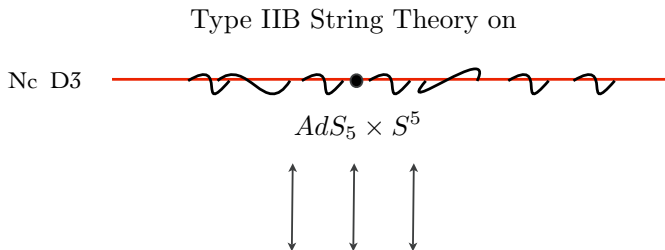
3 Berkooz-Douglas matrix model

- Quenched versus dynamical
- Low temperature holographic description
- High temperature expansion

AdS/CFT correspondence



AdS/CFT correspondence



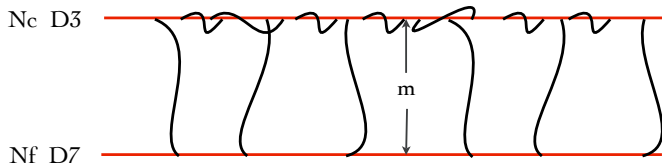
$$\mathcal{N} = 4 \, SU(N_c) \, \text{SUSY YM}$$

- Gubser-Klebanov-Polyakov-Witten formula:

$$\langle e^{\int d^d x \phi_0(x) \langle \mathcal{O}(x) \rangle} \rangle_{\text{CFT}} = \mathcal{Z}_{\text{string}}[\phi_0(x)]$$

Adding flavours

Generalizing the correspondence



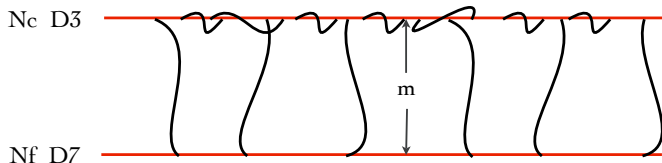
	0	1	2	3	4	5	6	7	8	9
D3	-	-	-	-
D7	-	-	-	-	-	-	-	-	.	.

- Adding N_f massive $\mathcal{N} = 2$ Hypermultiplets:

$$m_q \int d^2\theta \tilde{Q} Q \rightarrow \text{SYM} \quad \text{with} \quad m_q = m/2\pi\alpha'$$

Adding flavours

Generalizing the correspondence



	0	1	2	3	4	5	6	7	8	9
D3	-	-	-	-
D7	-	-	-	-	-	-	-	-	.	.

- Adding N_f massive $\mathcal{N} = 2$ Hypermultiplets:

$$m_q \int d^2\theta \tilde{Q} Q \rightarrow \text{SYM} \quad \text{with} \quad m_q = m/2\pi\alpha'$$

Probe approximation $N_f \ll N_c$

- The probe is described by a Dirac-Born-Infeld action

$$S \propto \int d^7\xi e^{-\Phi} \sqrt{||G_{ab} - 2\pi\alpha' \mathcal{F}_{ab}||}$$

Probe approximation $N_f \ll N_c$

- The probe is described by a Dirac-Born-Infeld action
$$\mathcal{S} \propto \int d^7\xi e^{-\Phi} \sqrt{||G_{ab} - 2\pi\alpha' \mathcal{F}_{ab}||}$$
- The profile of the D-brane encodes the fundamental condensate of theory. The semi-classical fluctuations correspond to meson-like excitations.

Probe approximation $N_f \ll N_c$

- The probe is described by a Dirac-Born-Infeld action
$$S \propto \int d^7\xi e^{-\Phi} \sqrt{||G_{ab} - 2\pi\alpha' \mathcal{F}_{ab}||}$$
- The profile of the D-brane encodes the fundamental condensate of theory. The semi-classical fluctuations correspond to meson-like excitations.
- The D-brane gauge field can describe: external electromagnetic field, chemical potential, electric current etc.

Probe approximation $N_f \ll N_c$

- The probe is described by a Dirac-Born-Infeld action
$$S \propto \int d^7\xi e^{-\Phi} \sqrt{||G_{ab} - 2\pi\alpha' \mathcal{F}_{ab}||}$$
- The profile of the D-brane encodes the fundamental condensate of theory. The semi-classical fluctuations correspond to meson-like excitations.
- The D-brane gauge field can describe: external electromagnetic field, chemical potential, electric current etc.
- Numerous applications: thermal and quantum phase transitions, chiral symmetry breaking, magnetic catalysis etc.

Probe approximation $N_f \ll N_c$

- The probe is described by a Dirac-Born-Infeld action
$$\mathcal{S} \propto \int d^7\xi e^{-\Phi} \sqrt{||G_{ab} - 2\pi\alpha' \mathcal{F}_{ab}||}$$
- The profile of the D-brane encodes the fundamental condensate of theory. The semi-classical fluctuations correspond to meson-like excitations.
- The D-brane gauge field can describe: external electromagnetic field, chemical potential, electric current etc.
- Numerous applications: thermal and quantum phase transitions, chiral symmetry breaking, magnetic catalysis etc.
- Can we test if AdS/CFT really works in this case?

Computer simulations of holographic gauge theories

- Using twisting techniques it seems possible to simulate $\mathcal{N} = 4$ $SU(N)$ SYM in $4D$ [S. Catterall, [hep-lat/0503036](#)], so far for small N .

Computer simulations of holographic gauge theories

- Using twisting techniques it seems possible to simulate $\mathcal{N} = 4$ $SU(N)$ SYM in $4D$ [S. Catterall, [hep-lat/0503036](#)], so far for small N .
- Not obvious how to generalise these techniques to include $\mathcal{N} = 2$ flavour hypermultiplet.

Computer simulations of holographic gauge theories

- Using twisting techniques it seems possible to simulate $\mathcal{N} = 4$ $SU(N)$ SYM in $4D$ [S. Catterall, [hep-lat/0503036](#)], so far for small N .
- Not obvious how to generalise these techniques to include $\mathcal{N} = 2$ flavour hypermultiplet.
- Consider instead 1D holographic gauge theories, which are super renormalizable.

Computer simulations of holographic gauge theories

- Using twisting techniques it seems possible to simulate $\mathcal{N} = 4$ $SU(N)$ SYM in 4D [S. Catterall, [hep-lat/0503036](#)], so far for small N .
- Not obvious how to generalise these techniques to include $\mathcal{N} = 2$ flavour hypermultiplet.
- Consider instead 1D holographic gauge theories, which are super renormalizable.
- Natural candidate is the D0/D4 system, T-dual to the D3/D7 and D3/D5 systems. (Same “class of universality”)

Computer simulations of holographic gauge theories

- Using twisting techniques it seems possible to simulate $\mathcal{N} = 4$ $SU(N)$ SYM in 4D [[S. Catterall, hep-lat/0503036](#)], so far for small N .
- Not obvious how to generalise these techniques to include $\mathcal{N} = 2$ flavour hypermultiplet.
- Consider instead 1D holographic gauge theories, which are super renormalizable.
- Natural candidate is the D0/D4 system, T-dual to the D3/D7 and D3/D5 systems. (Same “class of universality”)
- The field theory is the [Berkooz-Douglas](#) matrix model - a flavoured version of the [BFSS](#)-matrix model.

The BFSS matrix model

- It is the $\mathcal{N} = 16$ $SU(N)$ 1D SYM theory describing N D0-branes at low energy.

The BFSS matrix model

- It is the $\mathcal{N} = 16$ $SU(N)$ 1D SYM theory describing N D0-branes at low energy.
- It is conjectured to be a non-perturbative formulation of M-theory compactified on a circle. [T. Banks, W. Fischler, S. H. Shenker and L. Susskind: [hep-th/9610043](#)]

The BFSS matrix model

- It is the $\mathcal{N} = 16$ $SU(N)$ 1D SYM theory describing N D0-branes at low energy.
- It is conjectured to be a non-perturbative formulation of M-theory compactified on a circle. [T. Banks, W. Fischler, S. H. Shenker and L. Susskind: [hep-th/9610043](#)]
- Dimensionally reduce $\mathcal{N} = 1$ 10D SYM to 1D:

$$S_E = \frac{1}{g^2} \int d\tau \text{Tr} \left\{ \frac{1}{2} (D_\tau X^i)^2 - \frac{1}{4} [X^i, X^j]^2 + \frac{1}{2} \psi^T C_9 D_\tau \psi - \frac{1}{2} \psi^T C_9 \gamma^i [X^i, \psi] \right\} ,$$

The BFSS matrix model

- It is the $\mathcal{N} = 16$ $SU(N)$ 1D SYM theory describing N D0-branes at low energy.
- It is conjectured to be a non-perturbative formulation of M-theory compactified on a circle. [T. Banks, W. Fischler, S. H. Shenker and L. Susskind: [hep-th/9610043](#)]
- Dimensionally reduce $\mathcal{N} = 1$ 10D SYM to 1D:

$$S_E = \frac{1}{g^2} \int d\tau \text{Tr} \left\{ \frac{1}{2} (D_\tau X^i)^2 - \frac{1}{4} [X^i, X^j]^2 + \frac{1}{2} \psi^T C_9 D_\tau \psi - \frac{1}{2} \psi^T C_9 \gamma^i [X^i, \psi] \right\} ,$$

- The model enjoys a global $SO(9)$ symmetry and has flat directions associated to the Cartan modes:

$$[X^i, X^j] = 0$$

The BFSS matrix model

- The effective coupling is $g_{eff} = g^2 N U^{-3}$ and hence the model is UV free. A holographic description is only possible at low energies.

The BFSS matrix model

- The effective coupling is $g_{\text{eff}} = g^2 N U^{-3}$ and hence the model is UV free. A holographic description is only possible at low energies.
- The dual geometry is:

$$\begin{aligned} ds^2/\alpha' &= -H^{-1/2} dt^2 + H^{1/2} f^{-1} dU^2 + H^{1/2} U^2 d\Omega_8^2 \\ e^\Phi &= H^{3/4}, \quad C_{(1)} = H^{-1} dt \end{aligned}$$

- where:

$$H = \frac{L^7}{U^7}, \quad f = 1 - \frac{U_0^7}{U^7}, \quad U_0^5 = \left(\frac{4\pi}{7}\right)^2 L^7 T^2, \quad L^7 = 240\pi^5 \alpha'^5 \lambda, \quad \lambda = N g^2$$

The BFSS matrix model

- The effective coupling is $g_{\text{eff}} = g^2 N U^{-3}$ and hence the model is UV free. A holographic description is only possible at low energies.
- The dual geometry is:

$$\begin{aligned} ds^2/\alpha' &= -H^{-1/2} dt^2 + H^{1/2} f^{-1} dU^2 + H^{1/2} U^2 d\Omega_8^2 \\ e^\Phi &= H^{3/4}, \quad C_{(1)} = H^{-1} dt \end{aligned}$$

- where:

$$H = \frac{L^7}{U^7}, \quad f = 1 - \frac{U_0^7}{U^7}, \quad U_0^5 = \left(\frac{4\pi}{7}\right)^2 L^7 T^2, \quad L^7 = 240\pi^5 \alpha'^5 \lambda, \quad \lambda = N g^2$$

- Small curvature and string coupling require $1 \ll g_{\text{eff}} \ll N^{\frac{4}{7}}$.

- Lattice simulations (to the best of my knowledge):
 - Catterall & Wiseman, [0803.4273](#)
 - Kadoh & Kamata, [1503.08499](#)
 - Filev & O'Connor, [1506.01366](#)

- Lattice simulations (to the best of my knowledge):
 - Catterall & Wiseman, [0803.4273](#)
 - Kadoh & Kamata, [1503.08499](#)
 - Filev & O'Connor, [1506.01366](#)
- Non-lattice simulations:
 - First simulated by Anagnostopoulos, Hanada, Nishimura and Takeuchi [0707.4454](#)
 - The most extensive numerical studies of the BFSS model, providing non-trivial test of the AdS/CFT correspondence.

- Lattice simulations (to the best of my knowledge):
 - Catterall & Wiseman, [0803.4273](#)
 - Kadoh & Kamata, [1503.08499](#)
 - Filev & O'Connor, [1506.01366](#)
- Non-lattice simulations:
 - First simulated by Anagnostopoulos, Hanada, Nishimura and Takeuchi [0707.4454](#)
 - The most extensive numerical studies of the BFSS model, providing non-trivial test of the AdS/CFT correspondence.
- We focus on the studies performed in reference [1506.01366](#).

- Following Catterall and Wiseman we consider a basis in which $C_9 = \sigma_1 \otimes 1_8$ and discretise:

$$\begin{aligned}\psi^T C_9 \mathcal{D}_t \psi &\rightarrow (\psi_{1m}^T, \psi_{2m}^T) \cdot \begin{pmatrix} 0 & 1_8 (\mathcal{D}_-)^{mn} \\ 1_8 (\mathcal{D}_+)^{mn} & 0 \end{pmatrix} \cdot \begin{pmatrix} \psi_{1n} \\ \psi_{2n} \end{pmatrix} \\ \mathcal{D}_t X^i &\rightarrow \frac{U_{n,n+1} X_{n+1}^i U_{n+1,n} - X_n^i}{a}\end{aligned}$$

- where $(\mathcal{D}_\pm W)_n = \pm(U_{n,n\pm 1} W_{n\pm 1} U_{n\pm 1,n} - W_n)/a$

- Following Catterall and Wiseman we consider a basis in which $C_9 = \sigma_1 \otimes 1_8$ and discretise:

$$\begin{aligned}\psi^T C_9 \mathcal{D}_t \psi &\rightarrow (\psi_{1m}^T, \psi_{2m}^T) \cdot \begin{pmatrix} 0 & 1_8 (\mathcal{D}_-)^{mn} \\ 1_8 (\mathcal{D}_+)^{mn} & 0 \end{pmatrix} \cdot \begin{pmatrix} \psi_{1n} \\ \psi_{2n} \end{pmatrix} \\ \mathcal{D}_t X^i &\rightarrow \frac{U_{n,n+1} X_{n+1}^i U_{n+1,n} - X_n^i}{a}\end{aligned}$$

- where $(\mathcal{D}_\pm W)_n = \pm(U_{n,n\pm 1} W_{n\pm 1} U_{n\pm 1,n} - W_n)/a$
- The resulting lattice theory is free of fermion doubling.

- We employ the RHMC method [[hep-lat/0409133](#)] (Clark et al. 2004).

$$|\text{Pf}(\mathcal{M})| = \det(\mathcal{M}^\dagger \mathcal{M})^{1/4} \propto \int D\bar{\xi} D\xi e^{-\xi^\dagger (\mathcal{M}^\dagger \mathcal{M})^{-1/4} \xi}$$

- We employ the RHMC method [[hep-lat/0409133](#)] (Clark et al. 2004).

$$|\text{Pf}(\mathcal{M})| = \det(\mathcal{M}^\dagger \mathcal{M})^{1/4} \propto \int D\bar{\xi} D\xi e^{-\xi^\dagger (\mathcal{M}^\dagger \mathcal{M})^{-1/4} \xi}$$

- Define $S_{\text{ps.f}} \equiv \xi^\dagger (\mathcal{M}^\dagger \mathcal{M})^{-1/4} \xi$ and simulate $S_{\text{tot}} = S_{\text{bos}} + S_{\text{ps.f}}$

- We employ the RHMC method [[hep-lat/0409133](#)] (Clark et al. 2004).

$$|\text{Pf}(\mathcal{M})| = \det(\mathcal{M}^\dagger \mathcal{M})^{1/4} \propto \int D\bar{\xi} D\xi e^{-\xi^\dagger (\mathcal{M}^\dagger \mathcal{M})^{-1/4} \xi}$$

- Define $S_{\text{ps.f}} \equiv \xi^\dagger (\mathcal{M}^\dagger \mathcal{M})^{-1/4} \xi$ and simulate $S_{\text{tot}} = S_{\text{bos}} + S_{\text{ps.f}}$
- The idea is to approximate $(\mathcal{M}^\dagger \mathcal{M})^{-1/4}$ with a partial sum:

$$(\mathcal{M}^\dagger \mathcal{M})^\delta = \alpha_0 + \sum_{i=1}^{\#} \alpha_i (\mathcal{M}^\dagger \mathcal{M} + \beta_i)^{-1}$$

- We employ the RHMC method [hep-lat/0409133] (Clark et al. 2004).

$$|\text{Pf}(\mathcal{M})| = \det(\mathcal{M}^\dagger \mathcal{M})^{1/4} \propto \int D\bar{\xi} D\xi e^{-\xi^\dagger (\mathcal{M}^\dagger \mathcal{M})^{-1/4} \xi}$$

- Define $\mathcal{S}_{\text{ps.f}} \equiv \xi^\dagger (\mathcal{M}^\dagger \mathcal{M})^{-1/4} \xi$ and simulate $\mathcal{S}_{\text{tot}} = \mathcal{S}_{\text{bos}} + \mathcal{S}_{\text{ps.f}}$
- The idea is to approximate $(\mathcal{M}^\dagger \mathcal{M})^{-1/4}$ with a partial sum:

$$(\mathcal{M}^\dagger \mathcal{M})^\delta = \alpha_0 + \sum_{i=1}^{\#} \alpha_i (\mathcal{M}^\dagger \mathcal{M} + \beta_i)^{-1}$$

- The pseudo fermionic force is then:

$$\frac{\partial \mathcal{S}_{\text{ps.f}}}{\partial u} = - \sum_{i=1}^{\#} \alpha_i h_i^\dagger \frac{\partial (\mathcal{M}^\dagger \mathcal{M})}{\partial u} h_i ,$$

- where h_i satisfy $(\mathcal{M}^\dagger \mathcal{M} + \beta_i) h_i = \xi_i$ and can be obtained by a multi-shift solver.

- We study the following three observables:

- We study the following three observables:
 - Polyakov loop $P \equiv \frac{1}{N} \text{Tr} \mathcal{P} \exp \left(i \int_0^\beta dt A_0(t) \right)$

- We study the following three observables:

- Polyakov loop $P \equiv \frac{1}{N} \text{Tr} \mathcal{P} \exp \left(i \int_0^\beta dt A_0(t) \right)$
- Extend of space $\langle R^2 \rangle = \left\langle \frac{1}{N\beta} \int_0^\beta dt \text{Tr} (X^i)^2 \right\rangle$

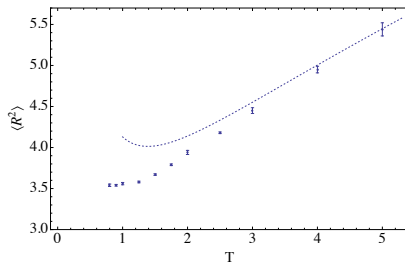
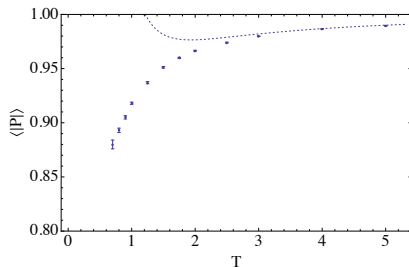
- We study the following three observables:

- Polyakov loop $P \equiv \frac{1}{N} \text{Tr} \mathcal{P} \exp \left(i \int_0^\beta dt A_0(t) \right)$
- Extend of space $\langle R^2 \rangle = \left\langle \frac{1}{N\beta} \int_0^\beta dt \text{Tr} (X^i)^2 \right\rangle$
- Internal energy $E/N^2 = -3T/N^2 (\langle S_{\text{bos}} \rangle - \frac{9}{2} \Lambda (N^2 - 1))$

- We study the following three observables:
 - Polyakov loop $P \equiv \frac{1}{N} \text{Tr} \mathcal{P} \exp \left(i \int_0^\beta dt A_0(t) \right)$
 - Extent of space $\langle R^2 \rangle = \left\langle \frac{1}{N\beta} \int_0^\beta dt \text{Tr} (X^i)^2 \right\rangle$
 - Internal energy $E/N^2 = -3T/N^2 (\langle S_{\text{bos}} \rangle - \frac{9}{2} \Lambda (N^2 - 1))$
- At high T we have theoretical predictions from the high T expansion considered in 0710.2188 (Kawahara et al. 2007)

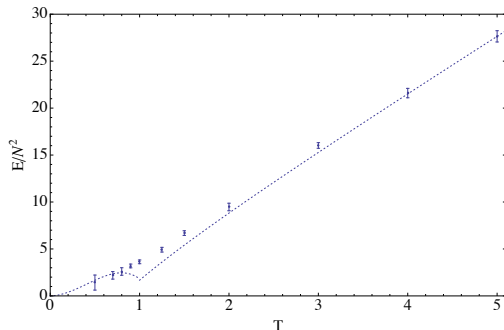
- We study the following three observables:
 - Polyakov loop $P \equiv \frac{1}{N} \text{Tr} \mathcal{P} \exp \left(i \int_0^\beta dt A_0(t) \right)$
 - Extent of space $\langle R^2 \rangle = \left\langle \frac{1}{N\beta} \int_0^\beta dt \text{Tr} (X^i)^2 \right\rangle$
 - Internal energy $E/N^2 = -3T/N^2 (\langle S_{\text{bos}} \rangle - \frac{9}{2} \Lambda (N^2 - 1))$
- At high T we have theoretical predictions from the high T expansion considered in 0710.2188 (Kawahara et al. 2007)
- At low T only the internal energy can be obtained from AdS/CFT

Results



- Plots of the expectation value of the Polyakov loop $\langle |P| \rangle$ and the extent of space $\langle R^2 \rangle$ as functions of temperature.
- The dashed curves represent the predictions of the high temperature expansion.
- Excellent agreement with the results of [0707.4454](#) and [1503.08499](#).

Results



- At high T the plot agrees with the predictions of [0710.2188](#). At low T the curve represents the AdS/CFT result including α' corrections:

$$\frac{1}{N^2} \frac{E}{\lambda^{1/3}} = \left(\frac{2^{21} 3^{12} 5^2}{7^{19}} \pi^{14} \right)^{1/5} \left(\frac{T}{\lambda^{1/3}} \right)^{14/5} - 5.58 \left(\frac{T}{\lambda^{1/3}} \right)^{23/5}$$

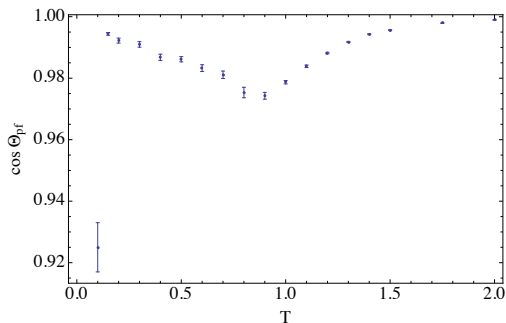
obtained in [0811.3102](#) (Hanada et al. 2008)

Sign Problem

- There is a special unitary transformation S transforming $C_9 \rightarrow 1_{16}$
- In this basis $\mathcal{M}(X) = \mathcal{M}_{kin} + \mathcal{M}_{pot}(X)$ with $\mathcal{M}_{kin}^\dagger = -\mathcal{M}_{kin}$ and $\mathcal{M}_{pot}(X)^\dagger = \mathcal{M}_{pot}(X)$
- Since $\mathcal{M}_{pot}(-X) = -\mathcal{M}_{pot}(X)$ it follows that $\mathcal{M}(-X) = -\mathcal{M}(X)^\dagger$ and therefore $\text{Pf}(\mathcal{M}(-\mathcal{X})) = \text{Pf}(\mathcal{M}(\mathcal{X}))^*$
- The symmetry $S_{\text{bos}}[-X] = S_{\text{bos}}[X]$ allows us to write:

$$\mathcal{Z} \propto \int \mathcal{D}X \text{Pf}(\mathcal{M}) e^{-S_{\text{bos}}[X]} = \int \mathcal{D}X \cos \Theta_{Pf} |\text{Pf}(\mathcal{M})| e^{-S_{\text{bos}}[X]}$$

- Now as long as $-\frac{\pi}{2} < \Theta_{Pf} < \frac{\pi}{2}$ the cosine is positive and the effective action defines a true probability distribution



- A plot of $\cos \Theta_{pf}$ for $N = 3$ and $\Lambda = 4$. The phase remains small for all T , but drops at very low temperatures possibly due to strong lattice effects.

Berkooz-Douglas matrix model

- Original motivation to introduce M_5 brane density to the BFSS matrix model [hep-th/9610236](#) (Berkooz & Douglas 1996).

Berkooz-Douglas matrix model

- Original motivation to introduce M_5 brane density to the BFSS matrix model [hep-th/9610236](https://arxiv.org/abs/hep-th/9610236) (Berkooz & Douglas 1996).
- Obtained by reducing the D5/D9 system (Van Raamsdonk, 2002):

$$\begin{aligned}\mathcal{L} = & \frac{1}{g^2} \text{Tr} \left(\frac{1}{2} D_0 X^a D_0 X^a + \frac{i}{2} \lambda^{\dagger \rho} D_0 \lambda_\rho + \frac{1}{2} D_0 \bar{X}^{\rho \dot{\rho}} D_0 X_{\rho \dot{\rho}} + \frac{i}{2} \theta^{\dagger \dot{\rho}} D_0 \theta_{\dot{\rho}} \right) \\ & + \frac{1}{g^2} \text{tr} \left(D_0 \bar{\Phi}^\rho D_0 \Phi_\rho + i \chi^\dagger D_0 \chi \right) + \mathcal{L}_{\text{int}}\end{aligned}$$

where:

$$\begin{aligned}\mathcal{L}_{\text{int}} = & \frac{1}{g^2} \text{Tr} \left(\frac{1}{4} [X^a, X^b] [X^a, X^b] + \frac{1}{2} [X^a, \bar{X}^{\rho \dot{\rho}}] [X^a, X_{\rho \dot{\rho}}] - \frac{1}{4} [\bar{X}^{\alpha \dot{\alpha}}, X_{\beta \dot{\alpha}}] [\bar{X}^{\beta \dot{\beta}}, X_{\alpha \dot{\beta}}] \right) \\ & - \frac{1}{g^2} \text{tr} \left(\bar{\Phi}^\rho (X^a - m^a) (X^a - m^a) \Phi_\rho \right) \\ & + \frac{1}{g^2} \text{tr} \left(\bar{\Phi}^\alpha [\bar{X}^{\beta \dot{\alpha}}, X_{\alpha \dot{\alpha}}] \Phi_\beta + \frac{1}{2} \bar{\Phi}^\alpha \Phi_\beta \bar{\Phi}^\beta \Phi_\alpha - \bar{\Phi}^\alpha \Phi_\alpha \bar{\Phi}^\beta \Phi_\beta \right) \\ & + \frac{1}{g^2} \text{Tr} \left(\frac{1}{2} \bar{\lambda}^\rho \gamma^a [X^a, \lambda_\rho] + \frac{1}{2} \bar{\theta}^{\dot{\alpha}} \gamma^a [X^a, \theta_{\dot{\alpha}}] - \sqrt{2} i \varepsilon_{\alpha \beta} \bar{\theta}^{\dot{\alpha}} [X_{\beta \dot{\alpha}}, \lambda_\alpha] \right) \\ & + \frac{1}{g^2} \text{tr} \left(\bar{\chi} \gamma^a (X^a - m^a) \chi + \sqrt{2} i \varepsilon_{\alpha \beta} \bar{\chi} \lambda_\alpha \Phi_\beta - \sqrt{2} i \varepsilon_{\alpha \beta} \bar{\Phi}^\alpha \bar{\lambda}_\beta \chi \right)\end{aligned}$$

Quenched versus dynamical

$$\begin{aligned}
 \bar{\lambda}^\alpha &\longleftrightarrow \lambda^\gamma \sim 1/N_c \\
 \Phi^\delta &\longleftrightarrow \bar{\Phi}^\beta \sim 1/N_c \\
 \chi &\longleftrightarrow \bar{\chi} \sim 1/N_c
 \end{aligned}
 \quad
 \begin{aligned}
 &\lambda^\gamma \longleftrightarrow \bar{\chi} \sim N_c \\
 &\Phi^\delta \longleftrightarrow \bar{\Phi}^\beta \sim N_c
 \end{aligned}$$

$$\begin{aligned}
 &\chi \longleftrightarrow \bar{\chi} \sim N_c \\
 &\Phi^\delta \longleftrightarrow \bar{\Phi}^\beta \sim N_c
 \end{aligned}
 =
 \begin{aligned}
 &\chi \longleftrightarrow \bar{\chi} \sim N_c \\
 &\Phi^\delta \longleftrightarrow \bar{\Phi}^\beta \sim N_c
 \end{aligned}$$

$$\text{Diagram} \sim N_f$$

$$\text{Diagram} \sim N_f$$

Quenched versus dynamical

- We conclude that we cannot quench the fundamental fermionic determinant.

Quenched versus dynamical

- We conclude that we cannot quench the fundamental fermionic determinant.
- We have two options:

Quenched versus dynamical

- We conclude that we cannot quench the fundamental fermionic determinant.
- We have two options:
 - Ignore the backreaction of the flavours on the adjoint fields and reweigh the fundamental determinant. Advantage: there is no extra sign problem. Disadvantage: it is computationally very expensive.

Quenched versus dynamical

- We conclude that we cannot quench the fundamental fermionic determinant.
- We have two options:
 - Ignore the backreaction of the flavours on the adjoint fields and reweigh the fundamental determinant. Advantage: there is no extra sign problem. Disadvantage: it is computationally very expensive.
 - Consider a full dynamical simulation. Advantage: easier to implement and execute. Disadvantage: There might be an extra sign problem.

Quenched versus dynamical

- We conclude that we cannot quench the fundamental fermionic determinant.
- We have two options:
 - Ignore the backreaction of the flavours on the adjoint fields and reweigh the fundamental determinant. Advantage: there is no extra sign problem. Disadvantage: it is computationally very expensive.
 - Consider a full dynamical simulation. Advantage: easier to implement and execute. Disadvantage: There might be an extra sign problem.
- We were able to show that in a dynamical simulation the path integral again depends only on $\cos \Theta_{Pf}$, which is an encouraging sign.

Holographic description

- In the probe approximation and at zero bare mass we obtain:

$$E = \left(\frac{3}{40}\right)^{1/5} \left(\frac{3\pi}{7}\right)^{8/5} N_f N_c \lambda^{1/3} \left(\frac{T}{\lambda^{1/3}}\right)^{8/5}$$

- In the probe approximation and at zero bare mass we obtain:

$$E = \left(\frac{3}{40}\right)^{1/5} \left(\frac{3\pi}{7}\right)^{8/5} N_f N_c \lambda^{1/3} \left(\frac{T}{\lambda^{1/3}}\right)^{8/5}$$

- At finite bare mass one has to obtain a numerical solution for the profile of the D4-brane.

- In the probe approximation and at zero bare mass we obtain:

$$E = \left(\frac{3}{40}\right)^{1/5} \left(\frac{3\pi}{7}\right)^{8/5} N_f N_c \lambda^{1/3} \left(\frac{T}{\lambda^{1/3}}\right)^{8/5}$$

- At finite bare mass one has to obtain a numerical solution for the profile of the D4-brane.
- The fact that the D0/D4 system lifts to a M_5 membrane with a KK-monopole suggests that a localised backreacted solution might be possible in analogy to the Cherkis-Hashimoto solution for the backreacted D2/D6 system.

High temperature expansion

- This is work in progress with D. O'Connor and Samuel Kovacik.

High temperature expansion

- This is work in progress with D. O'Connor and Samuel Kovacik.
- The first step is to expand the fields in furrier modes and scale the modes:

$$X_0 \rightarrow \beta^{-\frac{1}{4}} X_0, \quad A \rightarrow \beta^{-\frac{1}{4}} A,$$
$$(X, \Phi)_n \rightarrow \beta^{\frac{1}{2}} (X, \Phi)_n, \quad (\lambda, \theta, \chi)_n \rightarrow \beta^0 (\lambda, \theta, \chi)_n$$

treating the non-zero modes as fluctuations. In the extreme $T \rightarrow \infty$ limit only the zero modes survive and their action is given by the flavoured bosonic IKKT model.

High temperature expansion

- This is work in progress with D. O'Connor and Samuel Kovacik.
- The first step is to expand the fields in Fourier modes and scale the modes:

$$X_0 \rightarrow \beta^{-\frac{1}{4}} X_0, \quad A \rightarrow \beta^{-\frac{1}{4}} A,$$
$$(X, \Phi)_n \rightarrow \beta^{\frac{1}{2}} (X, \Phi)_n, \quad (\lambda, \theta, \chi)_n \rightarrow \beta^0 (\lambda, \theta, \chi)_n$$

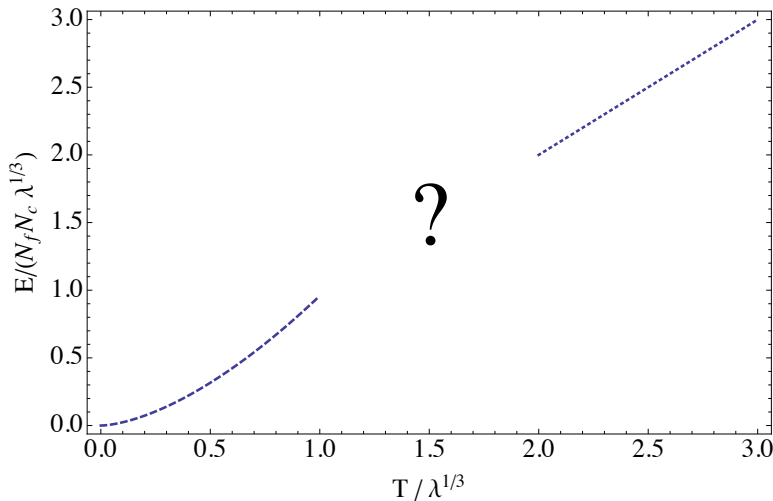
treating the non-zero modes as fluctuations. In the extreme $T \rightarrow \infty$ limit only the zero modes survive and their action is given by the flavoured bosonic IKKT model.

- For the energy one obtains:

$$E = N_f N_c \lambda^{1/3} T + \#_1 T^{1/2},$$

where $\#_1$ is a number that has to be determined from simulations of the flavoured bosonic IKKT model.

Goal



Summary

- We considered different types of flavoured holographic gauge theories.

Summary

- We considered different types of flavoured holographic gauge theories.
- We concluded that the most promising directions is to simulate the Berkooz-Douglas model.

Summary

- We considered different types of flavoured holographic gauge theories.
- We concluded that the most promising directions is to simulate the Berkooz-Douglas model.
- We performed independent lattice simulation of the BFSS model, confirming the results of previous such studies.

Summary

- We considered different types of flavoured holographic gauge theories.
- We concluded that the most promising directions is to simulate the Berkooz-Douglas model.
- We performed independent lattice simulation of the BFSS model, confirming the results of previous such studies.
- We argued that for the BFSS model the integrant in the partition function remains positive.

- We considered different types of flavoured holographic gauge theories.
- We concluded that the most promising directions is to simulate the Berkooz-Douglas model.
- We performed independent lattice simulation of the BFSS model, confirming the results of previous such studies.
- We argued that for the BFSS model the integrant in the partition function remains positive.
- We found that the probe limit $N_f \ll N_c$ does not suppress the fundamental determinant.

- We considered different types of flavoured holographic gauge theories.
- We concluded that the most promising directions is to simulate the Berkooz-Douglas model.
- We performed independent lattice simulation of the BFSS model, confirming the results of previous such studies.
- We argued that for the BFSS model the integrant in the partition function remains positive.
- We found that the probe limit $N_f \ll N_c$ does not suppress the fundamental determinant.
- We obtained the leading order behaviour of the energy at high and low T .

Thank you!